

Multilayer C₂N: Effect of Stacking Order and Number of Layers on Bandgap and Its Controlled Electronic Properties by External Electric Field

Ruiqi Zhang^a, Bin Li^a and Jinlong Yang^{a, b, *}

^a Hefei National Laboratory for Physical Sciences at Microscale, University of Science and Technology of China, Hefei, Anhui 230026, China

^b Synergetic Innovation Center of Quantum Information & Quantum Physics, University of Science and Technology of China, Hefei, Anhui 230026, China

KEYWORDS:

ABSTRACT

Successful synthesis of the nitrogenated holey two-dimensional structures C₂N (*Nat. Commun.* **2015**, *6*, 1–7) using simply wet-chemical reaction offer a cost-effective way to generate other 2D materials with novel optical and electronic properties. Using the few-layer C₂N as models, we have performed an ab initio study of electronic properties of layered C₂N. Band gaps of this system exhibit monotone decreasing as the number of layers increase. And a direct-gap to indirect-gap transition at the bulk C₂N. Besides, when we apply an out-of-plane electric field on few-layer C₂N, the band gap of multilayer C₂N will be decreased as the electric field increased

and a semiconductor-semimetal transition will happen for five-layer C₂N under an appropriate electric field, whereas the band gap of monolayer C₂N is unchanged under electric field. Owing to their tunable bandgaps in a wide range, layers C₂N will have tremendous opportunities to be applied in nanoscale electronic and optoelectronic devices.

1. INTRODUCTION

In recent years, two-dimensional (2D) materials are considered emerging ingredients for the future of nanoelectronics and optoelectronics applications due to their fascinating electronic, mechanical, optical or thermal properties.¹⁻³ Graphene, a hexagonal lattice of carbon atoms, have been attracted intensive research since its isolation one of the promising candidates for future applications in nanoscale electronics.⁴⁻⁶ However for graphene, the massless Dirac-fermion behavior make it possess extremely high mobility, but the absence of a fundamental band gap severely limits its applications in field-effect transistors.^{5,7,8} Then extensive efforts have been devoted to solve the problem of opening a gap in different graphene nanostructures.⁹ At the same time, a new class of 2D materials has been studied, such as few-layer transition metal dichalcogenides (TMDs),¹⁰⁻¹² and in particular MoS₂ does possess a direct bandgap of ~1.8 eV.¹⁰ Although monolayer MoS₂ has recently been used to fabricate a FET, the low carrier mobility¹³ of ~200 cm² V⁻¹ s⁻¹ limit its wide application in electronics. Recently, monolayer black phosphorous (phosphorene), with high mobility, high in-plane anisotropy and direct-bandgap semiconductor, was isolated from the bulk black phosphorus,¹⁴⁻¹⁷ which has immediately received considerable research attention.¹⁸⁻²² Although MoS₂ and phosphorene simultaneously satisfy appreciable band gap and high carrier mobility, their puckered lattices cannot strictly

confine the movement of the carrier within the 2D surface.²³ Thus, a search for 2D planer materials with a suitable stable bandgap is still ongoing.

Recently, a thinnest layered 2D crystal named C₂N, with uniform holes and nitrogen atoms, can be simply synthesized via a bottom-up wet-chemical reaction. Furthermore, a FET based on layer C₂N with an high on/off ratio of 10⁷ was fabricated and C₂N possess a optical bandgap of ~1.96 eV.²⁴ These results may make layer C₂N a very promising candidate material for future applications in nanoscale electronics and optoelectronics.

Here, we perform first-principles to investigate the electronic structures of few-layer and bulk C₂N resulting in several important findings. First, we found the monolayer C₂N with a direct band gap of ~1.66 eV at the Γ points based on our calculations. Besides, we explored the electronic properties of few-layer C₂N as a function of number layers. Our result show taht layer-C₂N exhibits a sizable and novel direct band gap, which is decreased as the number layers increased. What is more, when we explored how multilayers C₂N responses to a vertical electric field, we found the band gap of layer-C₂N are determined by the number of layer and the electric field intensity. With the number of layer and the electric field intensity increased, few-layer C₂N can be transform from a semiconductor to semimetal. All in all, the band gap of few-layer C₂N can be tuned in a relatively wide range, increasing the tunability for their potential application in nanoelectronics.

2. METHODS

In this study, our first-principles calculations are based on the density functional theory (DFT) implemented in the VASP package.^{25,26} The generalized gradient approximation of Perdew, Burke, and Ernzerhof (GGA-PBE)²⁷ and projector augmented wave (PAW) potentials are used. In all computations, the kinetic energy cutoff are set to be 520 eV in the plane-wave expansion.

For the geometry optimization, $5 \times 5 \times 1$ and $5 \times 5 \times 8$ Monkhorst-Pack k-meshes are adopted for the bulk and few-layer C_2N , respectively. A large value ~ 15 Å of the vacuum region is used to avoid interaction between two adjacent periodic images. All the geometry structures are fully relaxed until energy and forces are converged to 10^{-5} eV and 0.01 eV/Å, respectively. Dipole correction is employed to cancel errors of electrostatic potential, atomic forces and total energy, caused by periodic boundary condition. Effect of van der Waals (vdW) interaction is accounted for by using empirical correction method proposed by Grimme (DFT-D2),²⁸ which is a good description of long-range vdW interactions.^{22,29,30} As a benchmark, DFT-D2 calculations give an interlayer distance of 3.25 Å and a binding energy of -25 meV per carbon atom for bilayer graphene, consistent with previous experimental measurements and theoretical studies.^{31,32}

RESULTS AND DISCUSSION

To have a thorough knowledge of 2D C_2N , we first studied the geometric properties of monolayer C_2N . The atomistic ball-stick models of monolayer C_2N with a 2×2 supercell are illustrated in Fig. 1(a) and 1(b). Their plane structures are fully relaxed according to the force and stress calculated by DFT within the PBE functional, while the few-layer C_2N is obtained by the DFT-D2 method.

The equivalent lattice parameters of monolayer C_2N is 8.277 Å, generating the in-plane covalent bond lengths as C-C of 1.430 Å and C-N of 1.336 Å. Carefully looking at the geometric structures, we found there are 12 C atoms and 6 N atoms in a unite cell and uniform holes in the layer C_2N . By performing DFT-GGA calculations, it shown that a single layer C_2N is a semiconductor with a direct band gap of 1.66 eV at the Γ points, which is depicted in Fig. 1(c). At the same time, we plot the isosurfaces of band decomposed charge density corresponding to

the valence band maximum (VBM) and conduction band minimum (CBM), which is shown in Fig. 1(c) and (d), respectively. It is clear that the distribution of VBM and CBM is derived from different atoms: the former mainly originates from the nitrogen P_z states and the latter is mainly from the C=C antibonding π states.

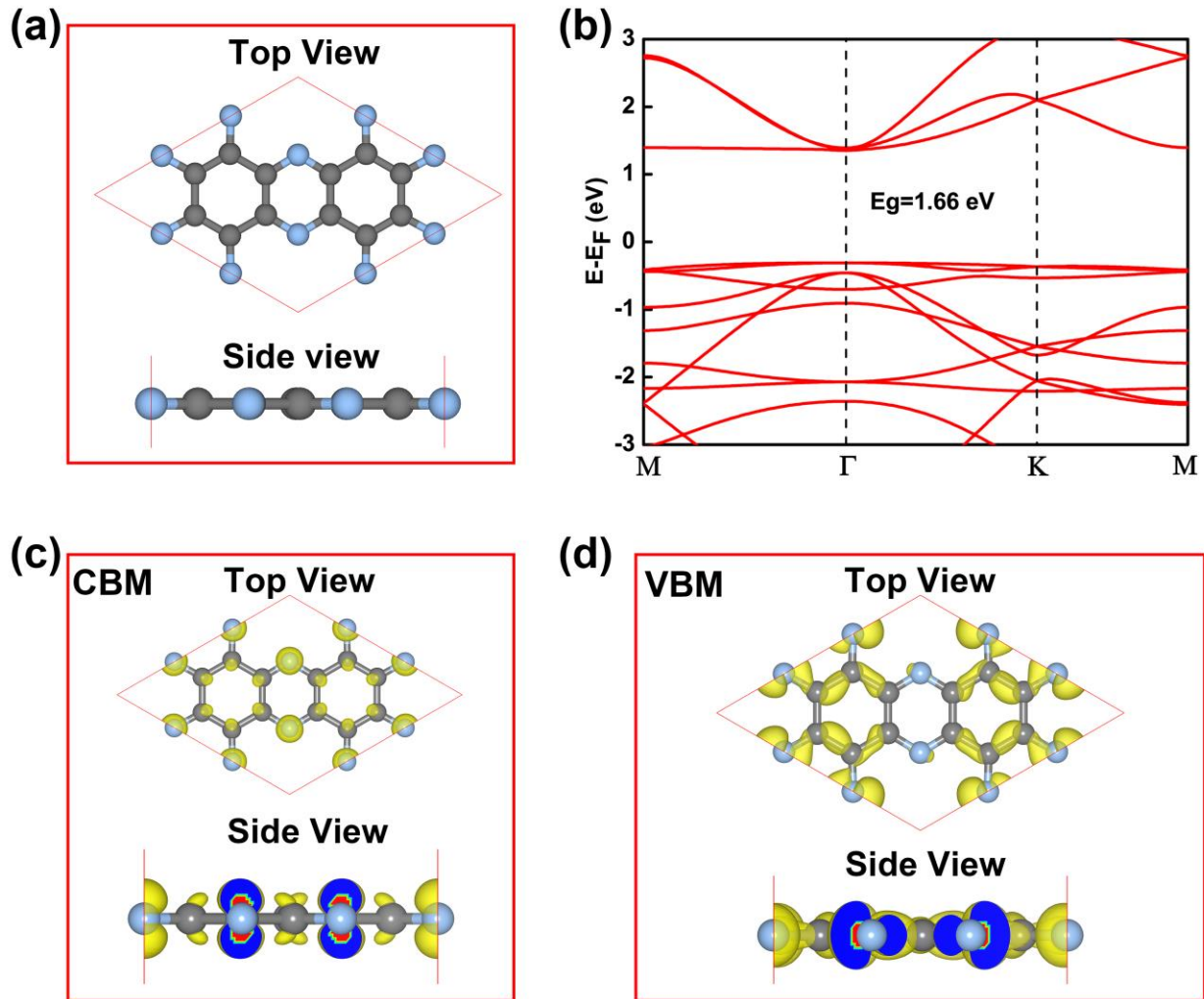


Figure 1. (a) Top view and side view of the atomic structure of monolayer C₂N. A 2×2 supercell is taken for brevity; (b) Band structures of monolayer C₂N calculated by PBE; (c,d) are the charge density corresponding to the CBM and VBM for monolayer, respectively. The isovalue is 0.003 e/Bohr^3 . The grey and silvery ball represent C atoms and N atoms, respectively.

Γ (0.0, 0.0, 0.0), M(0.5, 0.5, 0.0), and K (1/3, 1/3, 0.0) refer to special points in the first Brillouin zone.

To explore the bilayer C_2N , we considered three kinds of high symmetry stacking structures, namely, AA-, AB-, and AC-stacking. As shown in Fig. 2(a), for the AA-stacking, the top layer is directly stacked on the bottom layer. As for the AB-stacking, it is the C rings of the bottom layer that are under the center of the top layer holes. However, for the AC-stacking, it can be viewed as shifting the top layer of the AA-stacking by half of the cell along the basis vector, which result in the hexatomic rings composed by C and N atoms are just right under the center of the top layer holes. Our total energy calculations based on the PBE functional indicate that AB-stacking is the most favorable, which is 16 and 3 meV/atom lower than that of AA- and AC- stacking, respectively. Besides, we also note that the computed lattice constants differ slightly.

The PBE electronic band structures of AA-, AB-, and AC-stacked bilayer C_2N are shown in Fig. 3(d)–(f). Clearly, the direct-gap feature is retained regardless of the stacking orders. Both the VBM and CBM are located at the Γ point. Among the three bilayers with different stacking orders, the AB-stacked has the widest band gap of 1.49 eV. While the band gap of AA-, AB-stacked bilayer C_2N is 1.34 eV and 1.21 eV, respectively. Hence, it is different stacking-order results in different interactions between layers that makes different interaction strength and bandgap.

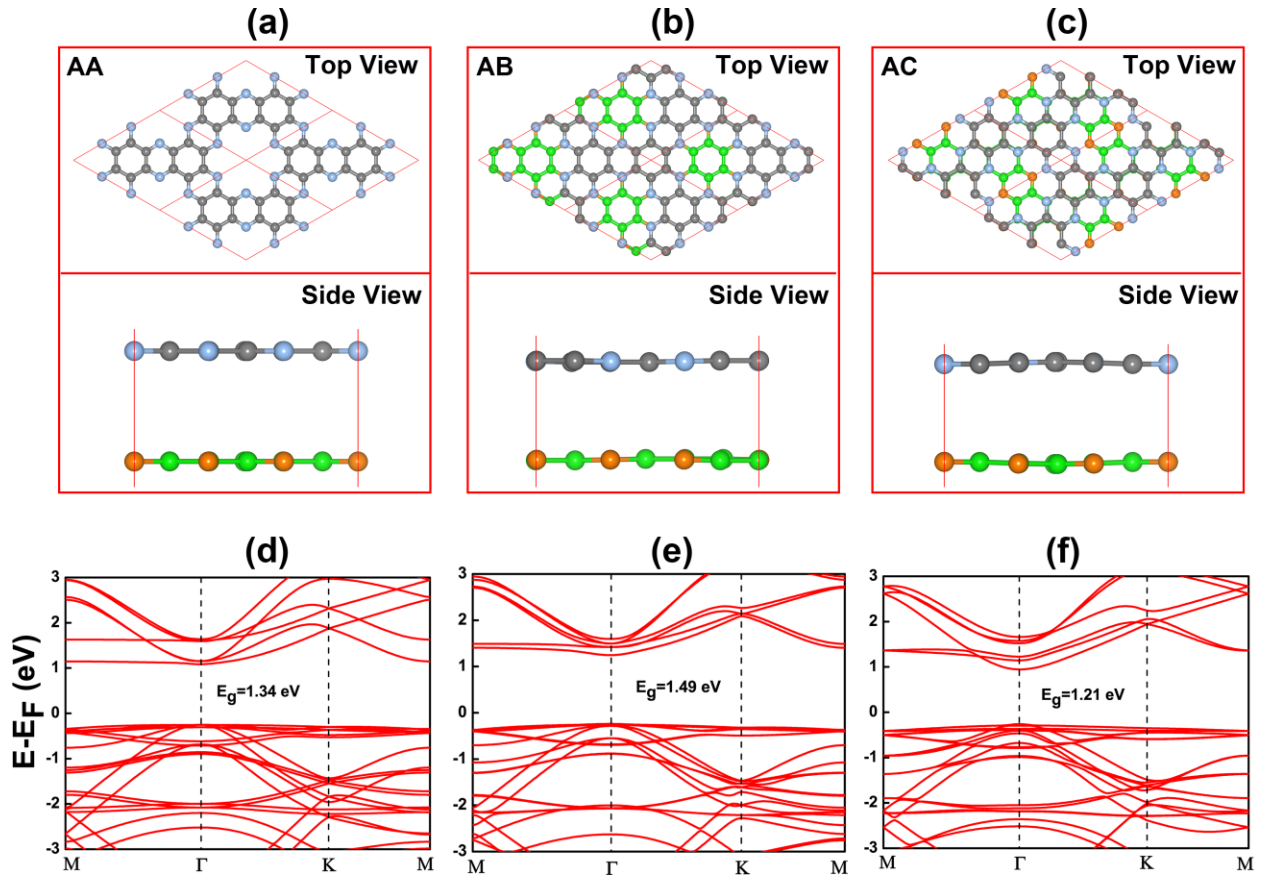


Figure 2. Three stacking structures of bilayer C_2N . (a,b,c) Top view and side view of AA-, AB-, and AC-stacking. A 2×2 supercell for top view is taken for brevity; (d,e,f) the electronic band structures of AA-, AB-, and AC-stacked bilayer C_2N , respectively. C atoms in different layers are represented by grey and green balls, respectively. And N atoms in different layers are represented by blue and orange balls, respectively. Γ (0.0, 0.0, 0.0), M(0.5, 0.5, 0.0), and K (1/3, 1/3, 0.0) refer to special points in the first Brillouin zone.

Then, we considered two stacking ways for trilayer C_2N based on AB-stacking: one is ABA stacking and the other one is ABC stacking. The difference between them is C can be considered as shifting A by half of the cell along the basis vector. The atomic structure of trilayer C_2N are

shown in Fig.4 (a) and (d), respectively. According to our total energy calculations, it is the ABC-stacking that has the more stable structure, which is 2 meV/atom lower than that of ABA-stacking. Then, their band structures are depicted in Fig. 4(b) and (e), respectively. Obviously, their band structures are almost same and suggest trilayer C₂N is a semiconductor with a direct bandgap. All their CBM and VBM are located in Γ point and the isosurfaces of the charge density corresponding to them are shown Fig. 4 (c) and (d).

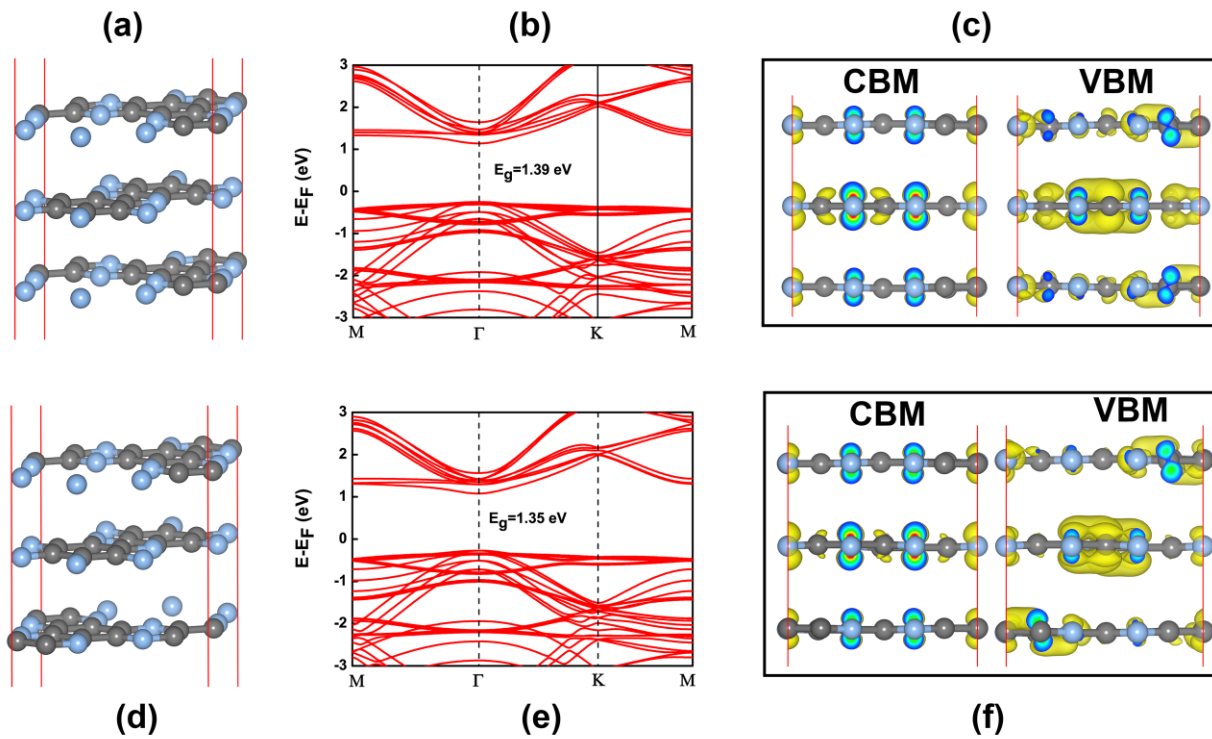


Figure 3. (a,d) The atomic structure of ABA- and ABC-stacked trilayer C₂N, respectively; (b,e) the electronic band structures of ABA- and ABC-stacked trilayer C₂N; (c) Side view of the charge density corresponding to the CBM and VBM for ABC-stacked. The isovalue is 0.003 e/Bohr³. The grey and silvery ball represent C atoms and N atoms, respectively. Γ (0.0, 0.0, 0.0), M(0.5, 0.5, 0.0), and K (1/3, 1/3, 0.0) refer to special points in the first Brillouin zone.

Then, we build multilayer even to bulk C₂N according to ABC–stacking. The calculated lattice (a) constant and the interlayer distance (Δc) are list in Table.2. The lattice parameter a decrease by 0.022 Å on passing from monolayer to bulk C₂N, whereas the interlayer distance Δc decrease by 0.054 Å from bilayer to bulk phase, which suggest the thicker the few-layer C₂N system the stronger is the interlayer interaction. While, the length of chemical bonding of C-N and C-C almost keep the same in the different layers.

Table.1 Lattice Constants a and Δc (Interlayer Distance) and the in-Plane Covalent Bond Lengths of Few-Layer C₂N Calculated Using DFT-D2

N _L	a (Å)	Δc (Å)	C-N (Å)	C-C(Å)
1	8.328		1.336	1.429/1.470
2	8.321	3.185	1.336	1.429/1.468
3	8.315	3.156	1.335	1.429/1.466
4	8.315	3.157	1.335	1.429/1.466
5	8.313	3.150	1.336	1.429/1.466
bulk	8.306	3.131	1.335	1.428/1.465

Another effect of layer increasing reflects on the band structures. To explore the reflects, we examine the electronic properties of few-layer C₂N nanosheets and find that the band gaps decrease as the number of layers increase, which is shown in Fig. 5(c). The few-layer C₂N has a

direct bandgap, tunable from 1.66 eV for a monolayer to 1.23 eV for a five-layer. However the bulk phase possess an in-direct bandgap with a value of 1.07 eV, whose atom atomic structure and band structure are shown in Fig.5 (a) and (b). Clearly, the CBM of bulk C_2N is located in A point and VBM is in Γ point.

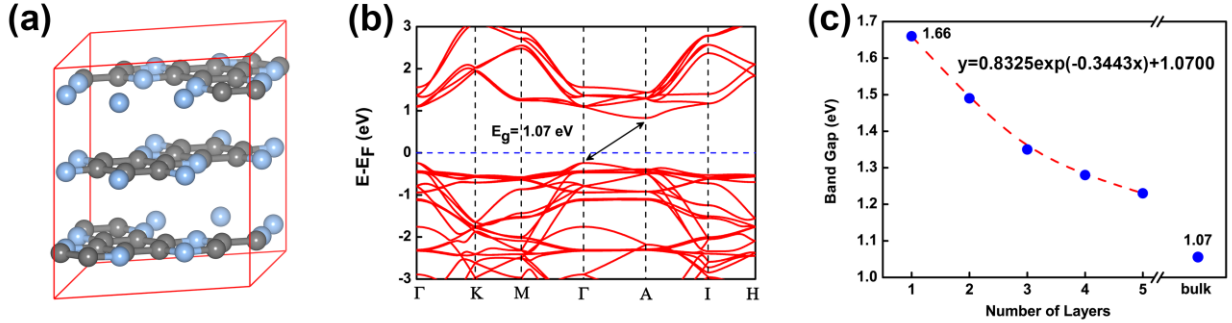


Figure 4. (a) Crystal structure of bulk C_2N ; (b) Band structures of bulk C_2N calculated by PBE.;(c) Evolution of the band gap of layer C_2N as a function of layer number.

Previous theoretical and experiment studies had showed that the external electric field may affect the bandgap of 2D materials.^{33–38} So it is interesting to study how few-layer C_2N responses to a vertical electric field. Then we choose the monolayer to five-layer C_2N as models to test. The electric field is applied perpendicular to the multilayer C_2N surface, with a strength ranging from 0.1 to 0.5 V/Å. For the monolayer, its band gap is almost unchanged as the external electric field increases. In contrast, the band gap of few-layer C_2N exhibit a monotonic decreasing relationship with increasing electrical field and close up as the electric field of 0.5 V/Å be applied in five-layer C_2N based on our PBE calculation, which is illustrated in Fig. 5(a) and (b). It is noted that the direct bandgap structures of our model with increasing electrical field are all kept until five-layer C_2N turn to a semimetal under the electric field of 0.5 V/Å. In order to explain why this transition happen in few-layer C_2N , we calculate their band structure. For

bilayer C_2N , it is clearly shown in Fig. 5(c) that CBM is derived from first layer and VBM is come from second layer. However, for five-layer C_2N , CBM is derived from the first layer and VBM is come from the bottom layer, which is shown in Fig. 5 (b). Compared with Fig. 5(c) and Fig. 5(d), the bands of bilayer C_2N are will kept in five-layer C_2N under the same electrical. It is clearly that the CBM get closer to the VBM as the value of electric field increase. It can be understood as bands shift for different layers happened under electric field, which is shown in Fig. 5(e). Then, when we plot the isosurfaces of the charge density corresponding to CBM and VBM of five-layer C_2N at Γ point. For example, when the strength of electric field get 0.4 V/\AA , the CBM almost comes from the first layer and VBM from the bottom layer, which is consistent with their band structures.

The above-discussed band gap modulation of few-layer C_2N under external electric field can be explained by Stark effect. Similar phenomenon has been observed in single-walled boron nitride nanotubes,^{39,40} boron nitride nanoribbons^{41,42} and MoS_2 bilayer.⁴³ When an external electric field is applied, the CBM and VBM in few-layer C_2N become localized at the two different edges. Owing to the external electrostatic potential difference between the two edges, the bands belonging to different C_2N layers are further split by the vertical electric field. As a result, the band gap is reduced with increased field strength and finally leads to a semiconductor to semimetal transition.

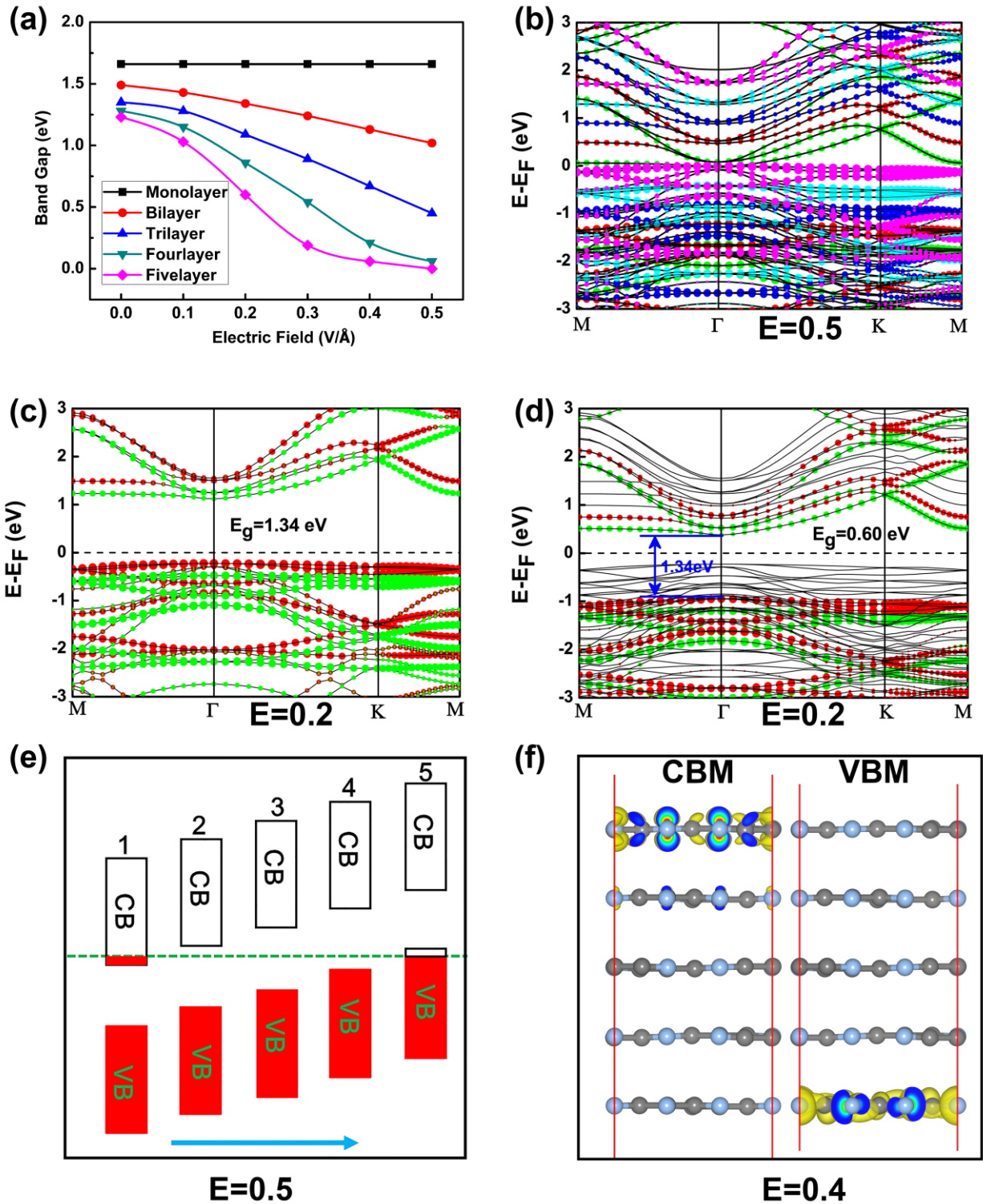


Figure 5. (a) Variations of band gap of layer C₂N under the external field; (b) Computed band structures (PBE) of five layer C₂N under electric field of 0.5 V/Å, bands of the first, second,

third, fourth and fifth layer are represented by green, red, blue, gray and magenta lines mark, respectively; Computed band structures (PBE) of (c) bilayer C_2N under electric field of 0.2 V/\AA , (d) five layer C_2N under electric field of 0.2 V/\AA , respectively. (e) A schematic view of bands shift for five-layer C_2N under electric field of 0.5 V/\AA , the green dotted line represents the Fermi level and the light blue arrow represents the direction of electric field. (f) the charge density corresponding to the CBM and VBM of five-layer C_2N under the electric fields of 0.4 V/\AA . The isovalue is 0.003 e/Bohr^3 .

IV. SUMMARY

In conclusion, on the basis of DFT calculations, we have performed a theoretical research on the structural and electronic properties of few-layer C_2N . We have shown theoretically that few-layer C_2N is a novel category of 2D direct band gap semiconductor, and the bandgap decreases as the number of layer increased. Owing to the band gap of multilayer C_2N are determined by edge states, when an external electric field perpendicular to the few-layer C_2N surface is applied, the bandgap of few-layer C_2N also decreases with increasing the vertical electric field and can be tuned in a relatively wide range, while for monolayer the band gap is unchanged. For example, under the electric field of 0.5 V/\AA , five-layer C_2N will tune to a semimetal, which can be explained by Stark effect. Thus, our theoretical predictions suggest that layer C_2N is very promising for optoelectronic applications, due to its tunable bandgaps by the number of layers and an external electric field, possible semiconductor to semimetal transition.

AUTHOR INFORMATION

Corresponding Author

* E-mail: jlyang@ustc.edu.cn. Phone: +86-551-63606408. Fax: +86-551-63603748 (J. Y.).

Author Contributions

The manuscript was written through contributions of all authors. All authors have given approval to the final version of the manuscript.

ACKNOWLEDGMENT

This work is partially supported by the National Key Basic Research Program (2011CB921404), by NSFC (21121003, 91021004, 21233007, 21203099, 21273210), by CAS (XDB01020300), and by USTCSCC, SCCAS, Tianjin, and Shanghai Supercomputer Centers.

REFERENCES

- (1) Xu, M.; Liang, T.; Shi, M.; Chen, H. Graphene-like Two-Dimensional Materials. *Chem. Rev.* **2013**, *113*, 3766–3798.
- (2) Butler, S. Z.; Hollen, S. M.; Cao, L.; Cui, Y.; Gupta, J. a.; Gutiérrez, H. R.; Heinz, T. F.; Hong, S. S.; Huang, J.; Ismach, A. F.; et al. Progress, Challenges, and Opportunities in Two-Dimensional Materials beyond Graphene. *ACS Nano* **2013**, *7*, 2898–2926.
- (3) Koski, K. J.; Cui, Y. The New Skinny in Two-Dimensional Nanomaterials. *ACS Nano* **2013**, *7*, 3739–3743.

- (4) Novoselov, K. S.; Geim, a. K.; Morozov, S. V.; Jiang, D.; Zhang, Y.; Dubonos, S. V.; Grigorieva, I. V.; Firsov, a. a. Electric Field Effect in Atomically Thin Carbon Films. *2004*, *306*, 666–669.
- (5) Schwierz, F. Graphene Transistors. *Nat. Nanotechnol.* **2010**, *5*, 487–496.
- (6) Geim, a K.; Novoselov, K. S. The Rise of Graphene. *Nat. Mater.* **2007**, *6*, 183–191.
- (7) Liao, L.; Lin, Y.-C.; Bao, M.; Cheng, R.; Bai, J.; Liu, Y.; Qu, Y.; Wang, K. L.; Huang, Y.; Duan, X. High-Speed Graphene Transistors with a Self-Aligned Nanowire Gate. *Nature* **2010**, *467*, 305–308.
- (8) Novoselov, K. S.; Geim, a K.; Morozov, S. V; Jiang, D.; Katsnelson, M. I.; Grigorieva, I. V; Dubonos, S. V; Firsov, a a. Two-Dimensional Gas of Massless Dirac Fermions in Graphene. *Nature* **2005**, *438*, 197–200.
- (9) Miró, P.; Audiffred, M.; Heine, T. An Atlas of Two-Dimensional Materials. *Chem. Soc. Rev.* **2014**, 6537–6554.
- (10) Mak, K. F.; Lee, C.; Hone, J.; Shan, J.; Heinz, T. F. Atomically Thin MoS₂: A New Direct-Gap Semiconductor. *Phys. Rev. Lett.* **2010**, *105*, 2–5.
- (11) Splendiani, A.; Sun, L.; Zhang, Y.; Li, T.; Kim, J.; Chim, C. Y.; Galli, G.; Wang, F. Emerging Photoluminescence in Monolayer MoS₂. *Nano Lett.* **2010**, *10*, 1271–1275.
- (12) Li, Y.; Zhou, Z.; Zhang, S.; Chen, Z. MoS₂ Nanoribbons: High Stability and Unusual Electronic and Magnetic Properties. *J. Am. Chem. Soc.* **2008**, *130*, 16739–16744.
- (13) Radisavljevic, B.; Radenovic, a; Brivio, J.; Giacometti, V.; Kis, a. Single-Layer MoS₂ Transistors. *Nat. Nanotechnol.* **2011**, *6*, 147–150.
- (14) Li, L.; Yu, Y.; Ye, G. J.; Ge, Q.; Ou, X.; Wu, H.; Feng, D.; Chen, X. H.; Zhang, Y. Black Phosphorus Field-Effect Transistors. *Nat. Nanotechnol.* **2014**, *9*, 372–377.
- (15) Liu, H.; Neal, A. T.; Zhu, Z.; Luo, Z.; Xu, X.; Tománek, D.; Ye, P. D. Phosphorene: An Unexplored 2D Semiconductor with a High Hole Mobility. *ACS Nano* **2014**, *8*, 4033–4041.
- (16) Xia, F.; Wang, H.; Jia, Y. Rediscovering Black Phosphorus as an Anisotropic Layered Material for Optoelectronics and Electronics. *Nat. Commun.* **2014**, *5*, 4458.
- (17) Qiao, J.; Kong, X.; Hu, Z.-X.; Yang, F.; Ji, W. High-Mobility Transport Anisotropy and Linear Dichroism in Few-Layer Black Phosphorus. *Nat. Commun.* **2014**, *5*, 4475.
- (18) Dai, J.; Zeng, X. C. Bilayer Phosphorene: E F f E ct of Stacking Order on Bandgap and Its Potential Applications in Thin-Film Solar Cells. **2014**, 2–6.

- (19) Liu, Q.; Zhang, X.; Abdalla, L. B.; Fazzio, A.; Zunger, A. Switching a Normal Insulator into a Topological Insulator via Electric Field with Application to Phosphorene. **2014**.
- (20) Fei, R.; Faghaninia, A.; Soklaski, R.; Yan, J. Enhanced Thermoelectric Efficiency via Orthogonal Electrical and Thermal Conductances in Phosphorene. *Nano Lett.* **2014**, *14*, 6393–6399.
- (21) Sun, J.; Zheng, G.; Lee, H. W.; Liu, N.; Wang, H.; Yao, H.; Yang, W.; Cui, Y. Formation of Stable Phosphorus-Carbon Bond for Enhanced Performance in Black Phosphorus Nanoparticle-Graphite Composite Battery Anodes. *Nano Lett.* **2014**, *14*, 4573–4580.
- (22) Zhang, R.; Li, B.; Yang, J. A First-Principles Study on Electron Donor and Acceptor Molecules Adsorbed on Phosphorene. *J. Phys. Chem. C* **2015**, *119*, 2871–2878.
- (23) Xie, J.; Zhang, Z. Y.; Yang, D. Z.; Xue, D. S.; Si, M. S. Theoretical Prediction of Carrier Mobility in Few-Layer BC₂N. **2014**.
- (24) Mahmood, J.; Lee, E. K.; Jung, M.; Shin, D.; Jeon, I.; Jung, S.; Choi, H.; Seo, J.; Bae, S.; Sohn, S.; et al. Nitrogenated Holey Two-Dimensional Structures. *Nat. Commun.* **2015**, *6*, 1–7.
- (25) Kresse, G.; Furthmüller, J. Efficiency of Ab-Initio Total Energy Calculations for Metals and Semiconductors Using a Plane-Wave Basis Set. *Comput. Mater. Sci.* **1996**, *6*, 15–50.
- (26) Kresse, G. Efficient Iterative Schemes for Ab Initio Total-Energy Calculations Using a Plane-Wave Basis Set. *Phys. Rev. B* **1996**, *54*, 11169–11186.
- (27) Perdew, J. P.; Burke, K.; Ernzerhof, M.; of Physics, D.; Quantum Theory Group Tulane University, N. O. L. 70118 J. Generalized Gradient Approximation Made Simple. *Phys. Rev. Lett.* **1996**, *77*, 3865–3868.
- (28) Grimme., S. Semiempirical GGA-Type Density Functional Constructed with a Long-Range Dispersion Correction. *J. Comput. Chem.* **2006**, *27*, 1787–1799.
- (29) Hu, W.; Wu, X.; Li, Z.; Yang, J. Porous Silicene as a Hydrogen Purification Membrane. *Phys. Chem. Chem. Phys.* **2013**, *15*, 5753–5757.
- (30) Hu, W.; Wu, X.; Li, Z.; Yang, J. Helium Separation via Porous Silicene Based Ultimate Membrane. *Nanoscale* **2013**, *5*, 9062–9066.
- (31) Baskin, Y.; Meyer, L. Lattice Constants of Graphite at Low Temperatures. *Phys. Rev.* **1955**, *100*, 544.
- (32) Zacharia, R.; Ulbricht, H.; Hertel, T. Interlayer Cohesive Energy of Graphite from Thermal Desorption of Polyaromatic Hydrocarbons. *Phys. Rev. B - Condens. Matter Mater. Phys.* **2004**, *69*, 1–7.

- (33) Ohta, T.; Bostwick, A.; Seyller, T.; Horn, K.; Rotenberg, E. Controlling the Electronic Structure of Bilayer Graphene. *Science* **2006**, *313*, 951–954.
- (34) Castro, E. V.; Novoselov, K. S.; Morozov, S. V.; Peres, N. M. R.; Dos Santos, J. M. B. L.; Nilsson, J.; Guinea, F.; Geim, a. K.; Neto, a. H. C. Biased Bilayer Graphene: Semiconductor with a Gap Tunable by the Electric Field Effect. *Phys. Rev. Lett.* **2007**, *99*, 8–11.
- (35) Oostinga, J. B.; Heersche, H. B.; Liu, X.; Morpurgo, A. F.; Vandersypen, L. M. K. Gate-Induced Insulating State in Bilayer Graphene Devices. *Nat. Mater.* **2008**, *7*, 151–157.
- (36) Mak, K. F.; Lui, C. H.; Shan, J.; Heinz, T. F. Observation of an Electric-Field-Induced Band Gap in Bilayer Graphene by Infrared Spectroscopy. *Phys. Rev. Lett.* **2009**, *102*, 100–103.
- (37) Ramasubramaniam, A.; Naveh, D.; Towe, E. Tunable Band Gaps in Bilayer Transition-Metal Dichalcogenides. *Phys. Rev. B - Condens. Matter Mater. Phys.* **2011**, *84*, 1–10.
- (38) Lu, N.; Guo, H.; Li, L.; Dai, J.; Wang, L.; Mei, W.-N.; Wu, X.; Zeng, X. C. MoS₂/MX₂ Heterobilayers: Bandgap Engineering via Tensile Strain or External Electrical Field. *Nanoscale* **2014**, *6*, 2879–2886.
- (39) Khoo, K.; Mazzoni, M.; Louie, S. Tuning the Electronic Properties of Boron Nitride Nanotubes with Transverse Electric Fields: A Giant dc Stark Effect. *Phys. Rev. B* **2004**, *69*, 1–4.
- (40) Ishigami, M.; Sau, J. D.; Aloni, S.; Cohen, M. L.; Zettl, a. Observation of the Giant Stark Effect in Boron-Nitride Nanotubes. *Phys. Rev. Lett.* **2005**, *94*, 1–4.
- (41) Park, C.-H.; Louie, S. G. Energy Gaps and Stark Effect in Boron Nitride Nanoribbons. *Nano Lett.* **2008**, *8*, 2200–2203.
- (42) Zhang, Z.; Guo, W.; Yakobson, B. I. Self-Modulated Band Gap in Boron Nitride Nanoribbons and Hydrogenated Sheets. *Nanoscale* **2013**, 6381–6387.
- (43) Liu, Q.; Li, L.; Li, Y.; Gao, Z.; Chen, Z.; Lu, J. Tuning Electronic Structure of Bilayer MoS₂ by Vertical Electric Field: A First-Principles Investigation. *J. Phys. Chem. C* **2012**, *116*, 21556–21562.